JOURNAL OF SOLID STATE CHEMISTRY **126,** 337–341 (1996)
ARTICLE NO. 0347

LETTER TO THE EDITOR

Magnetic Structure and Giant Magnetoresistance of Ferromagnetic $La_{1-\delta}Mn_{1-\delta}O_3$—An Example of Double-Exchange Striction?

A. K. Cheetham,* C. N. R. Rao,*,† and T. Vogt‡

*Materials Research Laboratory, University of California, Santa Barbara, California 93106; †Solid State and Structural Chemistry Unit, Indian Institute of Science, Bangalore 560012, India; and ‡Department of Physics, Brookhaven National Laboratory, Upton, New York 11973

Communicated by J. M. Honig, September 3, 1996; accepted September 5, 1996

A neutron powder diffraction study of the structure of the rhombohedral phase of $La_{1-\delta}Mn_{1-\delta}O_3$ ($\delta = 0.04$) as a function of temperature has been carried out. The crystal structure is well described at all temperatures by a model in $R-3c$ ($a = 5.52264(5)$ and $c = 13.3309(5)$ at 300 K) and the low temperature data contain magnetic contributions to the Bragg scattering due to ferromagnetic ordering below $T_c \sim 200$ K. The spin is canted at approximately 45° from [001]. The Mn–O–Mn angle decreases on cooling to T_c, but shows a slight increase on further cooling, presumably due to the onset of a double-exchange striction effect. Resistivity and magnetization data corroborate the neutron findings and reveal an insulator to metal transition close to T_c with a negative giant magnetoresistance value of ~50% at this temperature. The results confirm the striking similarity between the structural, magnetic, and conducting properties of rhombohedral $La_{1-\delta}Mn_{1-\delta}O_3$ and those of the solid solution $La_{1-x}A_xMnO_3$ ($x \sim 0.3$).

INTRODUCTION

The recent discovery of giant magnetoresistance (GMR) in the rare-earth manganates (1–5) $Ln_{1-x}A_xMnO_3$ (Ln = rare earth, A = a divalent cation such as Ca, Sr, Ba, Pb) with the perovskite structure has attracted considerable attention, not only because these oxides are new GMR systems but also because they exhibit several novel features. $LaMnO_3$ itself, as prepared by solid state reaction between the oxides and carbonates of the component metals, is an insulating perovskite with an orthorhombic structure (*Pbnm* (6)) and typically contains around 10% Mn^{4+}. $LaMnO_3$, with a smaller proportion of Mn^{4+} (<5%), becomes antiferromagnetically ordered below $T_N = 150$ K with an A-type magnetic structure (7). In the $La_{1-x}A_xMnO_3$ system, however, ferromagnetic behavior starts to manifest itself when x is ~0.1, and the compositions up to $x \sim 0.3$ have both antiferromagnetic and ferromagnetic characteristics (7). The $x = 0.3$ composition is purely ferromagnetic and exhibits strong GMR, while the $x > 0.5$ compositions are antiferromagnetic. The orthorhombic distortion in $La_{1-x}A_xMnO_3$ decreases as La is progressively replaced by a divalent ion, A, the material becoming rhombohedral ($R-3c$) and then cubic ($Fm3m$) as x increases.

The mechanism of incorporating Mn^{4+} into as-prepared $LaMnO_3$ has been examined in some detail. Since perovskites cannot accommodate excess oxygen, the defect chemistry of $LaMnO_3$ must involve the presence of cation vacancies in the La and Mn sites (8). Accordingly, $LaMnO_3$ is considered to be $La_{1-\delta}Mn_{1-\delta}O_3$. If the Mn^{4+} content in $LaMnO_3$ is 33%, for example, the formula will approximately correspond to $La_{0.945}Mn_{0.945}O_3$. The parent $LaMnO_3$ appears to mirror the behavior of the $La_{1-x}A_xMnO_3$ system, becoming rhombohedral and then cubic as the Mn^{4+} content is increased by chemical or electrochemical means (9, 10). The magnetic properties, too, are modified by increasing the concentration of Mn^{4+}, the antiferromagnetic structure of the orthorhombic $LaMnO_3$ giving way to ferromagnetism and GMR behavior in the rhombohedral phase (11). In the present work, we describe a neutron diffraction study of this rhombohedral phase as a function of temperature and present complementary magnetization and resistivity data.

EXPERIMENTAL

$LaMnO_3$ was prepared by the decomposition (at 500°C) of a gel obtained by treating a nitrate solution of La and Mn ions with citric acid and ethylenediamine. The product of the decomposition was first heated at 1200°C in air for 12 h and then at 930°C in a stream of oxygen for 12 h. The resulting $LaMnO_3$ had a rhombohedral structure. Redox titrations with $KMnO_4$ and ferrous sulfate showed the

0022-4596/96 $18.00

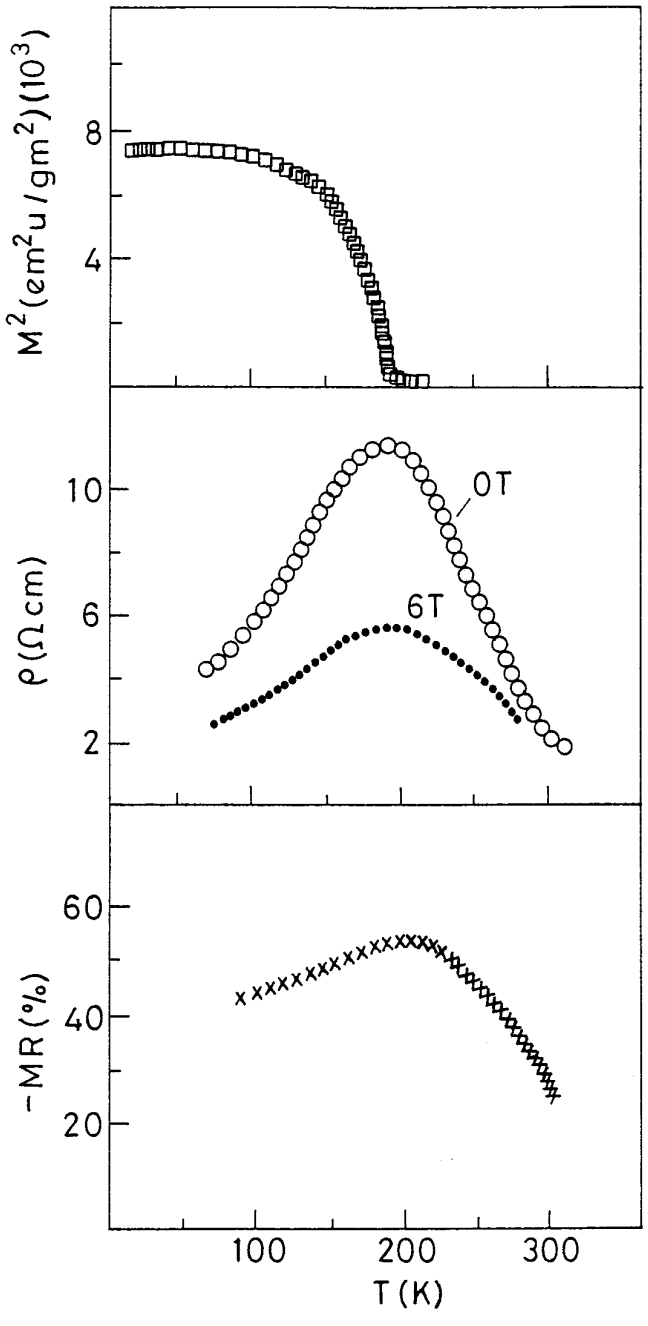

FIG. 1. The magnetization (M), resistivity (ρ), and magnetoresistance (MR) of $La_{1-\delta}Mn_{1-\delta}O_3$ as a function of temperature. MR data from (11).

Mn^{4+} content to be 25%. In terms of the defect structure, the stoichiometry can be written as $La_{0.96}Mn_{0.96}O_3$.

Electrical resistivity measurements were made in the 4.2–400 K temperature range using a four-probe technique. Magnetoresistance measurements were carried out in a maximum field of 6 T using a superconducting solenoid perpendicular to the direction of the current. Magnetization measurements were performed at 1 T.

Powder neutron diffraction data were collected on the new high resolution neutron powder diffractometer (HRNPD) at the High Flux Beam Reactor, Brookhaven National Laboratory. The instrument features a composite germanium monochromator (12) providing a neutron wavelength of 1.8857 Å. The sample was contained in a vanadium can and inserted into a two-stage displex (Air Products). The HRNPD is equipped with a detector bank consisting of 64 individual ^{3}He detectors separated by 2.5°

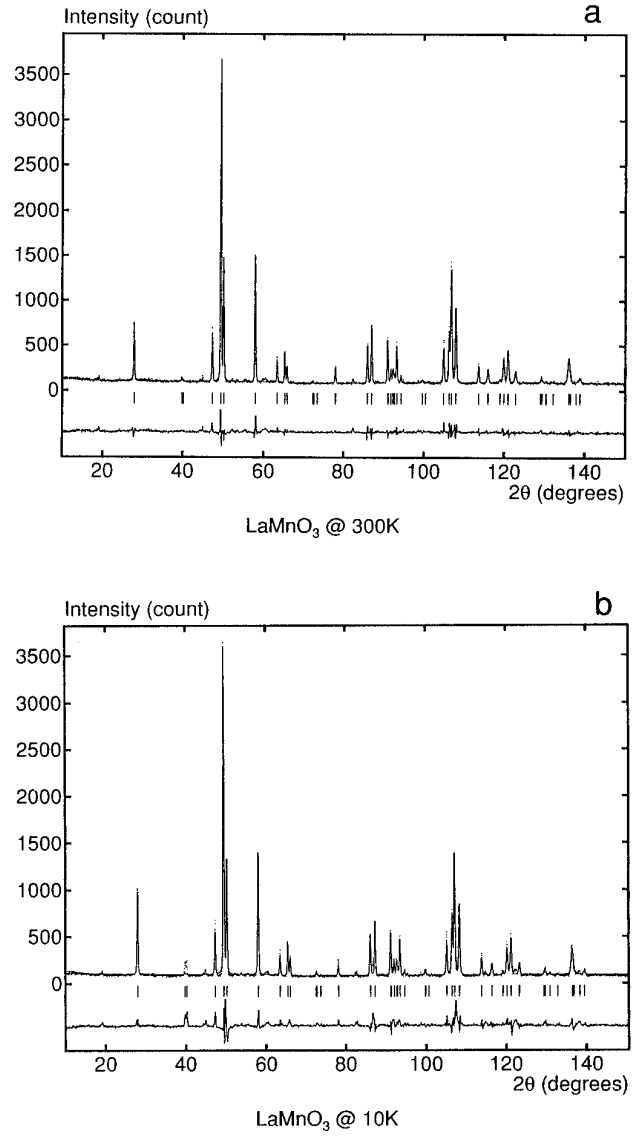

FIG. 2. The Rietveld refinement of $La_{1-\delta}Mn_{1-\delta}O_3$ at 300 K (a) and 10 K (b). Observed pattern, dots; calculated pattern, smooth curve; difference plot, lower curve. Tickmarks below show positions of nuclear Bragg peaks. The difference in (2b) is due to the magnetic scattering and was reduced by refining the magnetic model described in the text. Note, for example, the enhancement of the scattering in the doublet at ~40° 2Θ due to magnetic scattering.

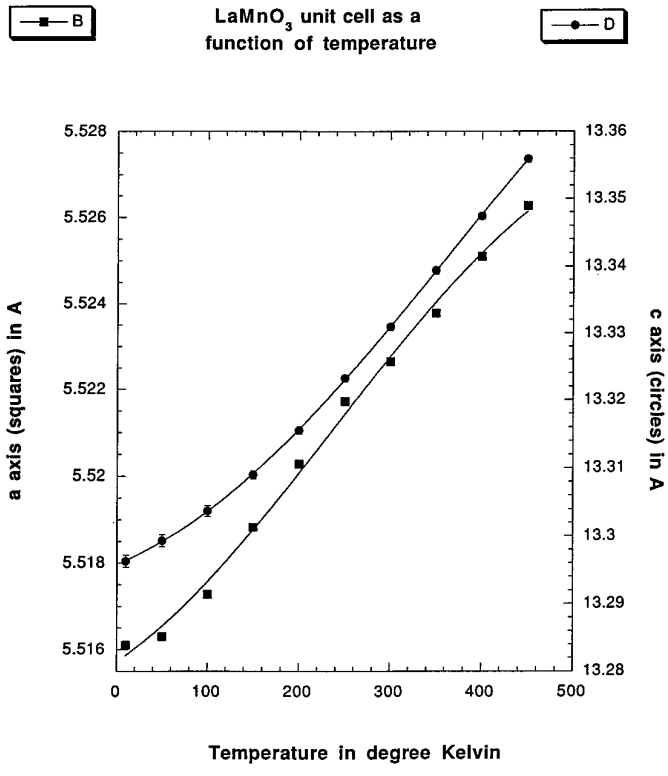

FIG. 3. The variation of the lattice parameters of $La_{1-\delta}Mn_{1-\delta}O_3$ as a function of temperature.

in 2Θ. The primary collimation used in front of the monochromator was 11′; the tertiary collimation is 5′ in front of the detectors. The entire detector bank was stepped at intervals of 0.05°.

The neutron diffraction data were analyzed by the Rietveld method (13), using the structure refinement program PROFIL (written by J. K. Cockroft); FULLPROF was used for the magnetic refinement (written by J. Rodriguez-Carvajal). A weighted average free-ion magnetic form factor for Mn^{3+}/Mn^{4+} was taken from Watson and Freeman (14).

RESULTS AND DISCUSSION

Figure 1 shows the magnetization data together with the temperature variation of the resistivity. The material becomes ferromagnetic on cooling, with T_c close to 200 K, and exhibits a insulator–metal transition close to this temperature. Application of a magnetic field of 6 T results in a considerable decrease in resistivity, the negative magnetoresistance reaching ~50% close to T_c, as reported earlier by Mahendiran *et al.* (11).

Excellent fits to the neutron diffraction data collected at 450, 400, 350, 300, 250, and 200 K were obtained using a rhombohedrally distorted perovskite structure (15) in space group $R-3c$ (Fig. 2). Atomic coordinates and other parameters are given in Table 1. However, data collected at temperatures below 200 K yielded poorer fits due to the appearance of weak but clearly discernible magnetic contributions to some of the low angle Bragg peaks (Fig.

TABLE 1
Table of Parameters for $La_{1-\delta}Mn_{1-\delta}O_3$ from Rietveld Refinement of Neutron Diffraction Data

	Space group $R-3c$	La at 6*a*	0, 0, 1/4
		Mn at 6*b*	0, 0, 0
		O at 18*e*	*x*, 0, 1/4

Temperature (K)	Oxygen *x*	R_{wp} (%)	X^2	μ (μ_B)
450	0.5503(4)	12.5	5.17	
400	0.5505(4)	12.6	5.25	
350	0.5508(4)	12.0	4.94	
300	0.5510(4)	11.8	4.77	
250	0.5514(4)	11.5	4.54	
200	0.5505(3)	12.2	5.10	
150	0.5506(3)	13.6	5.30	1.59(15)
100	0.5500(3)	11.4	4.60	2.25(13)
50	0.5494(4)	12.2	5.13	2.93(12)
10	0.55489(4)	13.6	5.30	3.21(12)

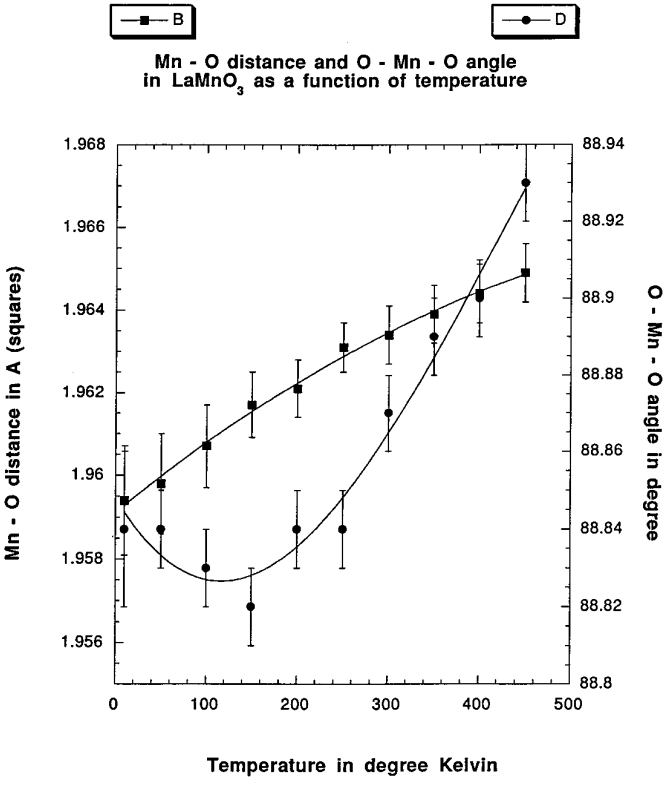

FIG. 4. The variation of the Mn–O distance (Å) and O–Mn–O angle (°) of $La_{1-\delta}Mn_{1-\delta}O_3$ as a function of temperature.

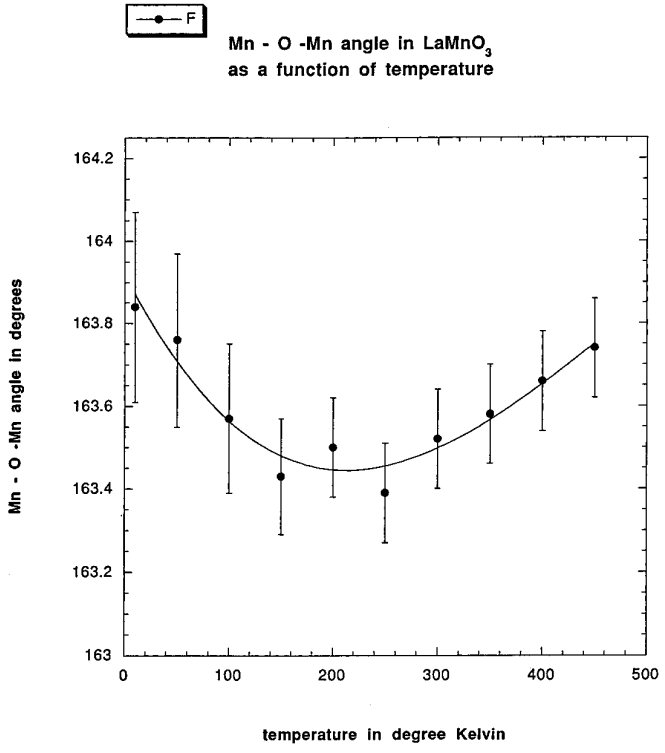

FIG. 5. The variation of the Mn–O–Mn angle (°) of $La_{1-\delta}Mn_{1-\delta}O_3$ as a function of temperature.

2b); this is particularly noticeable for the doublet of peaks at ~40° 2Θ. In light of the magnetization results (see above), the low temperature neutron data were therefore fitted to a model that included scattering due to ferromagnetic ordering of the spins; a good fit to the weak magnetic scattering intensity was found by using a canted-spin model with the spin fixed at 45° to [001]. A broadly similar model has recently been reported for the $La_{1-x}Sr_xMnO_{3+\delta}$ (x = 0.125) system (16).

The temperature variation of the unit cell parameters is shown in Fig. 3. There are no apparent discontinuities in the vicinity of T_c, confirming that the magnetic ordering transition is of second or higher order. The cell volumes, too, show no significant features in the vicinity of T_c. The temperature variations of the Mn–O bond length and O–Mn–O bond angle are shown in Fig. 4. The latter decreases steadily from 88.93 to 88.82 down to 150 K, but then levels off or perhaps shows a small increase. The onset of ferromagnetic ordering is therefore accompanied by a slight orthogonalization of the bonding around Mn, perhaps driven by the double-exchange mechanism (17) that is implicated in the itinerant electron behavior and ferromagnetism of the lanthanum manganates. The Mn–O–Mn bond angle shows a minimum in the vicinity of T_c, presumably for the same reason (Fig. 5). The system therefore exhibits what might be called ''double-exchange striction'' and shows clear evidence for coupling between the magnetic ordering and the crystal structure. We note that there is no Jahn–Teller distortion in the rhombohedral structure of $La_{1-\delta}Mn_{1-\delta}O_3$ since the point symmetry at the Mn site does not raise the degeneracy of the e_g level.

The temperature dependence of the observed magnetic moments in $La_{0.96}Mn_{0.96}O_3$ (Fig. 6) show the expected trends, with T_c close to 200 K, in agreement with the magnetization data; the absolute value of the moment at low temperatures (~3.2(1) μ_B) is in good agreement with the value of 3.32(7) μ_B reported in the $La_{1-x}Sr_xMnO_{3+\delta}$ (x = 0.125) system (16). Both c axis and in-plane components go to zero at T_c in our model, but the weakness of the magnetic data does not allow us to exclude other possible models such as that described by Argyriou *et al.*, in which the in-plane component is sustained above T_c (16).

ACKNOWLEDGMENTS

The work was funded by the MRL program of the National Science Foundation under Award DMR 9123048. The High Flux Beam Reactor at Brookhaven National Laboratory is supported by the U.S. Department of Energy, Basic Energy Science-Materials, under Contract De-AC02-76CH00016 (T.V.). We thank Dr. R. Mahesh for preparing the sample of $La_{1-\delta}Mn_{1-\delta}O_3$ and Dr. M. Verelst for some of the measurements.

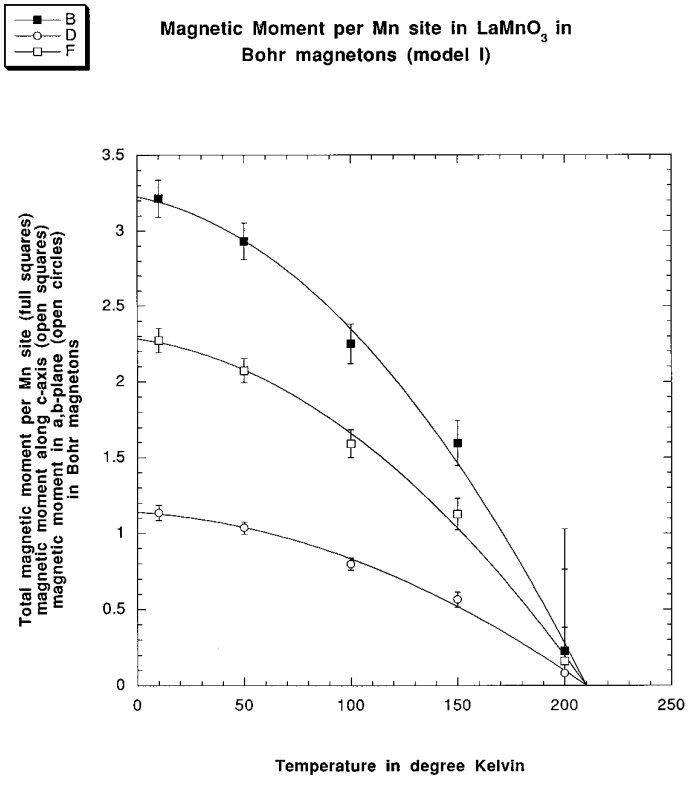

FIG. 6. The variation of the refined magnetic moment (μ_B) of $La_{1-\delta}Mn_{1-\delta}O_3$ as a function of temperature.

REFERENCES

1. M. N. Baibich, J. M. Broto, A. Fert, F. Nguyen Van Dau, F. Petroff, P. Etienne, G. Creuzet, A. Friederich, and Chazeles, *Phys. Rev. Lett.* **61,** 2472 (1988).
2. G. Binash, P. Grünberg, F. Saurenbach, and W. Zinn, *Phys. Rev. B* **39,** 4828 (1989).
3. (a) A. E. Berkowitz, J. R. Mitchell, M. J. Carey, A. P. Young, S. Zhang, F. E. Spada, F. T. Parker, A. Hatten, and G. Thomas, *Phys. Rev. Lett.* **68,** 3745 (1992); (b) P. Xiong, G. Xiao, J. Q. Wang, J. Q. Xiao, J. S. Jiang, and C. L. Chien, *Phys. Rev. Lett.* **69,** 3220 (1992).
4. (a) P. M. Levy, *Solid State Phys.* **47,** 367 (1994); (b) P. M. Levy and S. Zhang, *J. Mag. Magn. Mater.* **151,** 315 (1995).
5. C. N. R. Rao and A. K. Cheetham, *Science* **272,** 369 (1996).
6. J. B. A. A. Elemans, B. Van Laar, K. R. Van der Veen, and B. O. Loopstra, *J. Solid State Chem.* **3,** 238 (1971).
7. E. O. Wollan and W. C. Koehler, *Phys. Rev.* **100,** 545 (1955).
8. (a) J. A. M. van Roosmalen, E. H. P. Cordfunke, R. B. Helmholdt, and H. W. Zandbergen, *J. Solid State Chem.* **110,** 100 (1994); (b) J. A. M. van Roosmalen and E. H. P. Cordfunke, *J. Solid State Chem.* **110,** 109 (1994); (c) M. Hervieu, R. Mahesh, N. Rangavittal, and C. N. R. Rao, *Eur. J. Solid State Inorg. Chem.* **32,** 79 (1995); B. C. Tofield and W. R. Scott, *J. Solid State Chem.* **10,** 183 (1974).
9. R. Mahesh, K. R. Kannan, and C. N. R. Rao, *J. Solid State Chem.* **114,** 294 (1995).
10. J. A. Alonso, M. J. Martinez-Lope, and M. T. Casais, *Eur. J. Solid State Inorg. Chem.* **32,** 331 (1996).
11. (a) R. Mahendiran, R. Mahesh, N. Rangavittal, S. K. Tewari, A. K. Raychaudhuri, T. V. Ramakrishnan, and C. N. R. Rao, *Phys. Rev. B* **53,** 3348 (1996); (b) R. Mahendiran, R. Mahesh, A. K. Raychaudhuri, and C. N. R. Rao, *Pramana-J. Phys.* **44,** L393 (1995).
12. J. D. Axe, S. Cheung, D. E. Cox, L. Passell, T. Vogt, and S. Bar-Ziv, *J. Neutron Res.* **2,** 85 (1994); T. Vogt, L. Passell, S. Cheung, and J. D. Axe, *Nucl. Inst. Meth. A* **338,** 71 (1994).
13. H. M. Rietveld, *J. Appl. Crystallogr.* **2,** 65 (1969).
14. R. E. Watson and A. J. Freeman, *Acta Crystallogr.* **14,** 27 (1961).
15. A. Wold and R. J. Arnott, *J. Phys. Chem. Solids* **9,** 176 (1959).
16. D. N. Argyriou, J. F. Mitchell, C. D. Potter, D. G. Hinks, J. D. Jorgensen, and S. D. Bader, *Phys. Rev. Lett.* **76,** 3826 (1996).
17. C. Zener, *Phys. Rev.* **82,** 403 (1951); P. G. deGennes, *Phys. Rev.* **118,** 141 (1960).